Fault Detection and Isolation for a 3-DOF Helicopter with Sliding Mode Strategies

2018 15th International Workshop on Variable Structure Systems (VSS)
Graz University of Technology, Graz, Austria, July 9-11, 2018

Fault Detection and Isolation for a 3-DOF Helicopter with Sliding Mode Strategies

U. Pérez[1], E. Capello[2], E. Punta[3], J. Perea[1], and L. Fridman[1]

Abstract— **This paper analyzes the problem of detection and isolation of faults in the actuators of a 3-Degree-of-Freedom (3-DOF) helicopter by a residual-based approach. A third-order sliding mode differentiator is designed for the evaluation of the residuals. Moreover, two sliding mode controllers are suitably designed to stabilize the angular positions and velocities: (i) a super twisting control system and (ii) a continuous twisting control system. The performance of the designed controllers and the effectiveness of the residual-based method are illustrated by simulations.**

I. INTRODUCTION

In the last decades, due to the growing design of complex systems, the problem of fault detection and isolation (FDI) is one of the most important subject, mainly due to the need of increasing the productivity and the safety. The main objective of this paper is the identification and isolation of faults for a three Degree-of-Freedom (DOF) helicopter, combined with sliding mode controllers (SMCs) to partially or fully compensate these faults and to improve the performance of the studied system.

As proposed in [1], FDI techniques can be divided in three categories: (i) knowledge-based approach, (ii) signal processing-based approach, and (iii) analytical model-based approach. The first of this techniques strongly depends on the experience of the control operator, for example the expert system can use a combination of object-oriented modeling [2] or logic-based approach as in [3]. The second approach is based on the idea of hardware redundancy, this means that sensors measuring the same data are installed on-board to characterize off-line the fault. Drawbacks of this approach are related to the need of several measurements of the same data and that off-line computation cannot provide real time FDI. The interest on the third approach is increased in the last years due to the improvement on modeling techniques. This approach are considered efficient and easily applicable, as explained for example in [4] and [5]. The method proposed in this paper is based on this last approach, since the mathematical model of the system is well known and differentiator-based approach is considered to deduce the faults informations. The model-based methods of fault detection were developed by using input and output signals and applying dynamic process models. In detail, as presented in [5], these methods are based, e.g., on parameter estimation, parity equations or state observers. Moreover, fault diagnosis is typically achieved by combining a residual generator and a residual evaluation strategy to provide Boolean decisions on whether faults have occurred. Marzat et.a. [6] presented a survey of model-based fault diagnosis, which focuses on those methods that are applicable to aerospace systems.

Since some of the electromechanical parameters are uncertain during operations, SMC is a general method for designing controllers for uncertain systems and provides invariance to matched uncertainties, that is, uncertainties that affect the dynamics of the system acting in the input channels and insensitivity to parameters variations. The main features of SMC are the robustness properties against matched and bounded external disturbances and parameter variations, as well as the simplicity in design. The main advantages of these controllers are high precision, robustness and finite time convergence. In [7] the authors show how SMCs can be exploited for fault detection (specifically fault signal estimation) and subsequently fault tolerant control, including an aerospace application. An appropriate combination of the adopted SMC and sliding mode differentiator (SMD) is considered in [6] and this algorithms combination is designed to on-line detect and reconstruct the faults and also to give a sensorless control strategy which can achieve tolerance to a wide class of total additive failures.

The main objectives of this paper are: (i) to detect and isolate faults in the actuators of a three degrees of freedom (3-DOF) helicopter [8], and (ii) to implement a reconctructive fault-tolerant control. The FDI technique is based on the theory of both Super Twisting (STW) control and Continuous Twisting Algorithm (CTA). Moreover, the faults in the actuation system are compensated by the CTA controller [9]. Further, a third-order sliding mode differentiator is designed for the estimation of the angular velocities and accelerations to evaluate the missing data in the state vector and to construct the residual equations. The present paper continues the research initiated in [10]. The novelties of this paper are: (i) the design of two SMC control schemes for the system dynamics control, (ii) both fault detection and fault-tolerant control are proposed, and (iii) one of the proposed controller is able to compensate faults in the actuators.

The paper has the following structure. In Section II the problem and the 3-DOF helicopter model is presented. Section III is dedicated to the control design of the two

[1]L. Fridman, J. Perea and U. Pérez are with National Autonomous University of Mexico, Department of Control and Robotics, Division of Electrical Engineering, Engineering Faculty, C.P. 04510, D.F., Mexico, lfridman@unam.mx

[2]E. Capello is with the Department of Mechanical and Aerospace Engineering, Politecnico di Torino and with CNR-IEIIT, Corso Duca degli Abruzzi 24, 10129 Torino, Italy, elisa.capello@polito.it

[3] E. Punta is with the Institute of Electronics, Computer and Telecommunication Engineering, National Research Council of Italy (CNR-IEIIT), Torino, Italy (elisabetta.punta@ieiit.cnr.it), and with the International Telematic University UniNettuno, Rome, Italy.

proposed controller schemes (STW SMC and CTA SMC). The residual equations are given in Section IV. Extensive simulation results are presented in Section V. Finally, some concluding remarks are in Section VI.

II. PROBLEM STATEMENT

The main idea of this paper is to make a comparison between of the two proposed controllers, when a failure in the actuators occurs. Moreover, the performance of both controller are compared in terms of exact compensation, not only in terms of detection and isolation.

The following 3-DOF helicopter model (Figure 1) is analyzed. The range of the parameter variation is in Table II and the parameters given by the manufacturer are in the Table II.

$$\begin{aligned}\ddot{\varepsilon} &= \frac{g}{J_\varepsilon}\left(M_w L_w - M_h L_a\right) + \frac{K_f L_a}{J_\varepsilon} u_s \\ \ddot{\rho} &= \frac{K_f L_h}{J_\rho} u_d \\ \ddot{\theta} &= \frac{-K_p L_a}{J_\theta} \sin\left(\rho\right)\end{aligned} \tag{1}$$

The state vector is $x = \begin{bmatrix}\varepsilon & \rho & \theta & \dot{\varepsilon} & \dot{\rho} & \dot{\theta}\end{bmatrix}^T$, where ε and $\dot{\varepsilon}$ are related to the elevation dynamics, ρ, and $\dot{\rho}$ are related to the pitch dynamics, whereas θ and $\dot{\theta}$ are related to the travel angle dynamics. The control input $u = \begin{bmatrix}u_s & u_d\end{bmatrix}^T$ is defined according to the voltages in the engines. So, we have that $u_s = V_f + V_b$ and $u_d = V_f - V_b$, with V_f voltage in front engine and V_b voltage in back engine, assuming that these voltages are proportional to the lift forces $F_f = K_f u_d$ and $F_b = K_f u_s$, by a constant K_f, respectively for the front and back engines. The gravity force is $F_g = \frac{g}{J_\varepsilon}\left(M_w L_w - M_h L_a\right)$. All the parameters are defined in Table II.

The control system (1) can be rewritten as follows, where the elevation and pitch-travel dynamics are kept separated

$$\ddot{\varepsilon} = \begin{bmatrix}0 & 1 \\ 0 & 0\end{bmatrix}\begin{bmatrix}\varepsilon \\ \dot{\varepsilon}\end{bmatrix} + \begin{bmatrix}0 \\ \frac{K_f L a}{J_\varepsilon}\end{bmatrix} u_s + F_g, \tag{2}$$

$$\begin{bmatrix}\ddot{\rho} \\ \ddot{\theta}\end{bmatrix} = \begin{bmatrix}0 & 1 & 0 & 0 \\ 0 & 0 & 0 & 0 \\ 0 & 0 & 0 & 1 \\ \frac{-K_p L a}{J_\theta}\sin\left(\rho\right) & 0 & 0 & 0\end{bmatrix}\begin{bmatrix}\rho \\ \dot{\rho} \\ \theta \\ \dot{\theta}\end{bmatrix} + \begin{bmatrix}0 \\ \frac{K_f L_h}{J_\rho} \\ 0 \\ 0\end{bmatrix} u_d. \tag{3}$$

TABLE I
WORKSPACE AND SIGNAL CONTROL

Variable	Value	Units	Description
ε	$[-25,\ 25]$	Degree	Elevation position
ρ	$[-90,\ 90]$	Degree	Pitch position
θ	$[-\infty, \infty]$	Degree	Travel position
V_f	$[-15, 15]$	V	Voltage in front engine
V_b	$[-15, 15]$	V	Voltage in back engine

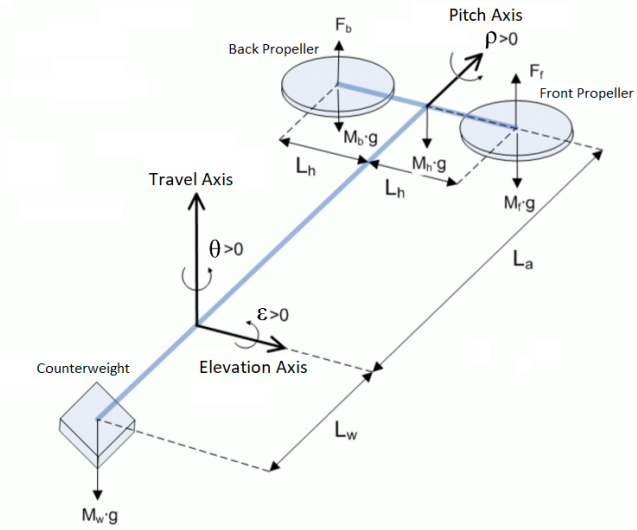

Fig. 1. Free-body diagram for 3-DOF helicopter

TABLE II
MODEL PARAMETERS

Parameter	Value	Units	Description
J_ρ	0.0364	kgm^2	Inertial moment around the pitch axis
J_ε	0.91	kgm^2	Inertial moment around the elevation axis
J_θ	0.91	kgm^2	Inertial moment around the travel axis
K_p	0.686	N	Flight constant
K_f	0.5	N/V	Voltage-Force propellers constant
M_h	1.15	kg	Helicopter mass
M_w	1.87	kg	Counterweight mass
L_a	0.66	m	Helicopter-elevation axis length
L_h	0.177	m	Propeller-pitch axis length
L_w	0.47	m	Counterweight-elevation axis length
g	9.81	m/s^2	Gravitational constant

III. CONTROL DESIGN

Two control schemes are proposed for stabilizing the trajectories of the system (Figure 1) in the equilibrium point $\begin{bmatrix}\varepsilon & \rho & \theta\end{bmatrix}^T = [0, 0, 0]^T$. Moreover, this equilibrium point represents the initial condition. This means that, if a fault occurs, the controller is able to compensate it exactly.

1) Super Twisting Control: The super-twisting (STW) [11] sliding mode control strategy is based on a second order sliding mode controller. The STW sliding mode controller designs a continuous control, thus reducing the chattering phenomenon and therefore the mechanical stress since no discontinuous control variations are required. Furthermore, STW SMC results to be easy to implement and guarantees high performance and efficiency.

For the design of super twisting algorithm the following sliding surfaces are proposed

$$\begin{aligned}S_1 &= c_1\varepsilon + \dot{\varepsilon}, \\ S_2 &= -B_2\dot{\rho}\cos\rho - 3c_2 B_2 \sin\rho + 3c_2^2\dot{\theta} + c_2^3\theta.\end{aligned} \tag{4}$$

where $B_2 = \frac{-K_p L_a}{J_\theta}$ and the sliding variables (4) are defined such that the zero-dynamics of the system (2)-(3) on $S_1 = S_2 = 0$ is asymptotically stable. The sliding surface

S_2 is defined as in [10].

The control u_s can be written as

$$u_s = \frac{J_\varepsilon}{K_f L_a}\left(-k_1|S_1|^{\frac{1}{2}}\text{sgn}\,(S_1) + v_1\right), \qquad \dot{v}_1 = -k_2\text{sgn}\,(S_1) \tag{5}$$

and the control u_d as

$$u_d = \frac{J_\rho}{K_f L_h}\left(-k_3|S_2|^{\frac{1}{2}}\text{sgn}\,(S_2) + v_2\right). \qquad \dot{v}_2 = -k_4\text{sgn}\,(S_2) \tag{6}$$

2) Continuous Twisting Algorithm: The Continuous Twisting Algorithm (CTA) [9] is a homogeneous control algorithm for uncertain second order plants. CTA designs continuous control signals, is able to compensate Lipschitz uncertainties/perturbations, and guarantees finite-time convergence to third-order sliding mode.

As shown in Section II, the 3-DOF helicopter can be decoupled in two subsystems: (i) one related to the elevation dynamics and (ii) one related to the pitch dynamics; both are second order systems.

For the design of continuous twisting algorithm the following sliding surfaces are proposed

$$\begin{aligned} S_1 &= \varepsilon, \\ S_2 &= c_3\frac{-K_p L_a}{J_\theta}\sin(\rho) + c_4\theta + c_5\dot{\theta}. \end{aligned} \tag{7}$$

where the gains c_3, c_4 and c_5 of the sliding variable (7) are chosen such that both zero dynamics ($s_2 = 0$) are asymptotically stable.

The structure of the control u_s is as follows

$$u_s = \frac{J_\varepsilon}{K_f L_a}\left(-K_1|S_1|^{\frac{1}{3}}\text{sgn}(S_1) - K_2|\dot{S}_1|^{\frac{1}{2}}\text{sgn}(\dot{S}_1) + \eta_1\right), \qquad \dot{\eta}_1 = -K_3\text{sgn}(S_1) - K_4\text{sgn}(\dot{S}_1) \tag{8}$$

and the structure for u_d is

$$u_d = \frac{J_\rho}{K_f L_h}\left(-K_5|S_2|^{\frac{1}{3}}\text{sgn}(S_2) - K_6|\dot{S}_2|^{\frac{1}{2}}\text{sgn}(\dot{S}_2) + \eta_1\right). \qquad \dot{\eta}_1 = -K_7\text{sgn}(S_2) - K_8\text{sgn}(\dot{S}_2) \tag{9}$$

IV. FAULT DETECTION AND ISOLATION

For the identification of faults, the required information is related to the angular accelerations. To achieve this information in finite time, third-order differentiators are designed, which also provide the velocity values for the control system. See Figure 2 for the connection scheme.

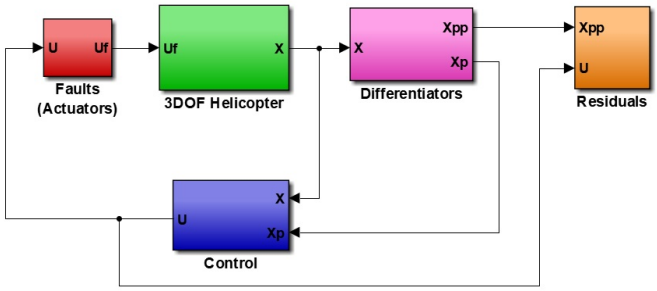

Fig. 2. Control scheme

A. Actuators faults

Actuators faults represent a partial loss or total loss of the actuators control action. The actuators faults of helicopters mainly include constant output faults, constant gain change faults and drift faults. Constant gain faults represent that the actual output values of actuators are γ, $0 \leq \gamma \leq 1$, percent of the normal case, like servo power and main rotor power lost their efficiency. In this paper we consider this kind of actuator faults. There are two cases: (i) fault of the front motor (V_f) and (ii) fault of the back motor (V_b).

The fault of the front motor is defined as follows

$$V_f^* = \begin{cases} V_f & if \quad t < t_f \\ \gamma_f V_f & if \quad t \geq t_f \end{cases} \tag{10}$$

In Eq. (10) the fault occurs in a fault time t_f and it is represented as a scaled value of the front engine voltage by means of a constant gain γ_f. V_f^* is the new value of the front engine voltage, V_f is the assigned front engine voltage and $0 < \gamma_f < 1$ is a constant value, which expresses the percentage of fault.

In a similar way, the fault of the back engine is represented in Eq. (11).

$$V_b^* = \begin{cases} V_b & if \quad t < t_b \\ \gamma_b V_b & if \quad t \geq t_b \end{cases} \tag{11}$$

As before, V_b^* is the new value of the back engine voltage, V_b is the assigned back engine voltage and $0 < \gamma_b < 1$ is a constant value, which expresses the percentage of fault. More details about fault definition are given in [1] and [10].

Let us consider the vector of the outputs available to the controller and some of its derivatives in order to establish later on the residual generator and the corresponding FDI approach.

We define the following vector $Y(t)$

$$Y(t) = [\ddot{\varepsilon} \quad \ddot{\rho} \quad \ddot{\theta}]^T, \tag{12}$$

and each component (i.e. angular accelerations) of the vector $Y(t)$ can be exactly estimated in finite time using robust exact third-order sliding mode differentiators as in [12].

B. Residual Method

The main idea of the residual method, once the system is stabilized, is to identify deviations in the accelerations,

to identify faults in each engines, as shown below. The following cases are considered:

- Fault in the front engine:

$$\begin{aligned} \ddot{\varepsilon} &= F_g + \frac{K_f L_a}{J_\varepsilon}\left(u_s + \delta_f\right), \\ \delta_f &= -\left(1-\gamma_f\right) V_f \text{sgn}\left(V_f\right) \end{aligned} \tag{13}$$

- Fault in back engine:

$$\begin{aligned} \ddot{\rho} &= \frac{K_f L_h}{J_\rho}\left(u_d - \delta_b\right) \\ \delta_b &= -\left(1-\gamma_b\right) V_b \text{sgn}\left(V_b\right) \end{aligned} . \tag{14}$$

The residual equations are designed according to [10].

Remark 1: As can be seen in Eq. (13)) the fault represents a change in the control coefficient, affecting V_f, while in Eq. (14)) the affected coefficient is V_b. These expressions allow to isolate the faults in the actuators (engines) of the system.

The residual-based equations can be defined as

$$R_\varepsilon = A_1\left(\ddot{\varepsilon} - F_g\right) - u_s, \tag{15}$$

and

$$R_\rho = A_2\ddot{\rho} - u_d, \tag{16}$$

with $A_1 = \frac{J_\varepsilon}{K_f L_a}$, $A_2 = \frac{J_\rho}{K_f L_h}$, $u_s = V_f + V_b$ and $u_d = V_f - V_b$.

Remark 2: Starting from Eq. (15) and Eq. (16) the fault can be detected (if it occurred in the front engine or the back engine).

V. SIMULATIONS RESULTS

Simulations have been done in the Matlab Simulink environment, employ the Euler discretization method with a fixed sampling time $\tau = 10^{-4}$ $[s]$. The initial conditions for all simulations are $x(0) = \begin{bmatrix} 2 & 1 & -0.5 & 0 & 0 & 0 \end{bmatrix}$, the duration of the simulations is $T = 40$ $[s]$.

An intermittent fault occurs in the front motor (10), in the interval of time $T_f = [t_{f_1}, t_{f_2}]$ with $t_{f_1} = 10$ $[s]$ and $t_{f_2} = 20$ $[s]$. In the interval T_f the tension of front motor fall as $\gamma_f = 0.85$ which represents about 15% of the nominal voltage. After the interval T_f the fault vanishes, i.e. $\gamma_f = 1$. On the other hand, a persistent fault occurs in the back motor (11) at the time $t_b = 30$ $[s]$, the tension of back motor fall as $\gamma_b = 0.9$ which represents about 10% of the nominal voltage. Firstly, the results obtained by simulations for the STA control law are analyzed, and then the CTA closed-loop is tested.

1) Results for Super Twisting Control: The gains employed for the surface in (4) is $c_1 = 1$ and $c_2 = 1$ which ensure zero dynamics asymptotically stable. The gains for the control u_s in (5) are $k_1 = 2.2$ and $k_2 = 0.9$. The gains for u_d in (6) are proposed as $k_3 = 2.2$ and $k_4 = 0.9$.

It can be seen from Fig. 3 that all the states have been the settling time about 5 $[s]$ from the initial conditions to the equilibrium point $X = \begin{bmatrix} 0 & 0 & 0 & 0 & 0 & 0 \end{bmatrix}^T$. The faults (variation of the voltage in any of the engines) are compensated exactly by the ST controller. The controllers

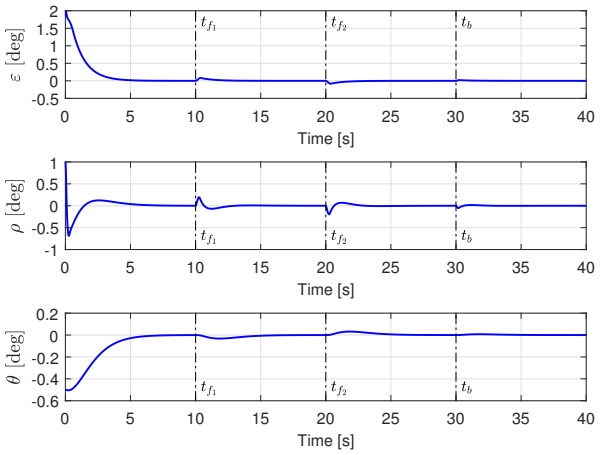

Fig. 3. Angular positions of the 3-DOF Helicopter in closed-loop with ST control.

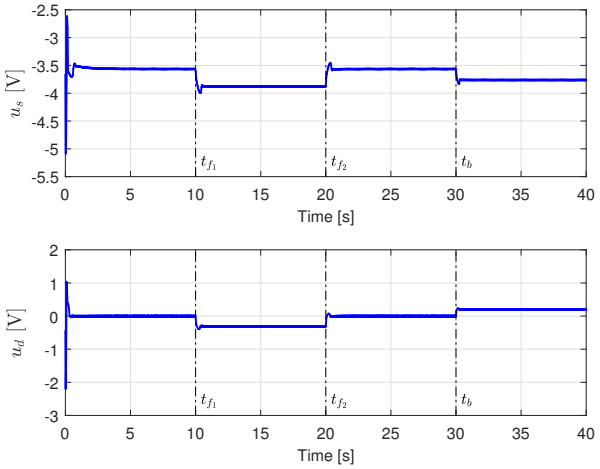

Fig. 4. Super-Twisting Controllers.

u_s in (5) and u_d in (6) are drawing in Fig. 4. There are proportional changes in the magnitude of the controllers when any fault occurs.

The residual equations (15) and (16) are shown in Fig. 5. It can be note when a fault occurs in the front motor (interval T_f) both residual equations have the same magnitude and sign. On the other hand, when a fault occurs in the back motor (at the time t_b until the end) both residual equations have the same magnitude but opposite sign.

2) Results for Continuous Twisting Control: The gains employed for the surface in (7) are $c_3 = 0.4113$, $c_4 = -0.9920$ and $C_4 = -1.8187$ which ensure zero dynamics asymptotically stable. The gains for the control u_s in (8) are $K_1 = 1.2$, $K_2 = 2.4$, $K_3 = 0.2$ and $K_4 = 0$. The gains for u_d in (9) are proposed as $K_5 = 1.2$, $K_6 = 2.4$, $K_7 = 0.2$ and $K_8 = 0$.

It can be seen from Fig. 6 that all the states have been the settling time about 5 $[s]$ from the initial conditions to the equilibrium point $X = \begin{bmatrix} 0 & 0 & 0 & 0 & 0 & 0 \end{bmatrix}^T$. We can note that the faults (fall of voltage in any of the engines) are

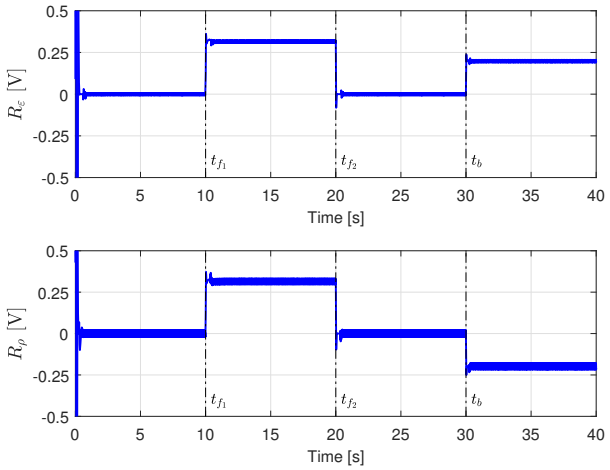

Fig. 5. Fault detection with ST control.

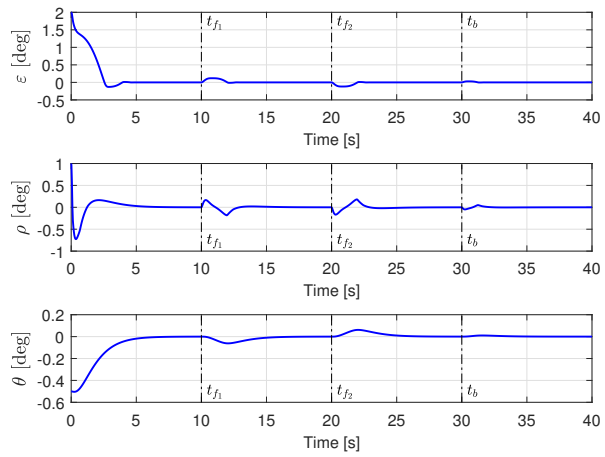

Fig. 6. Angular position of the 3-DOOF Helicopter in closed-loop with CTA control.

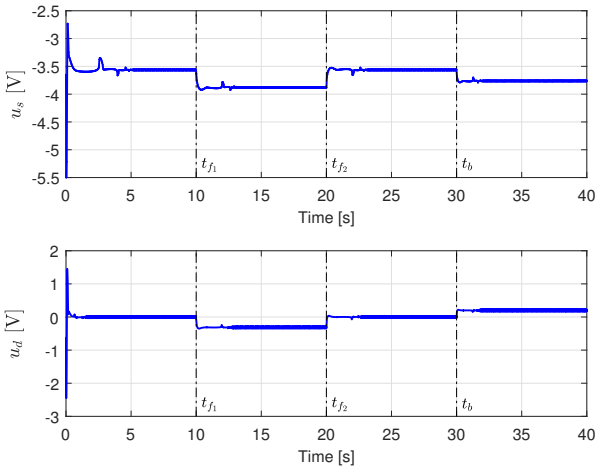

Fig. 7. Super-Twisting Controllers.

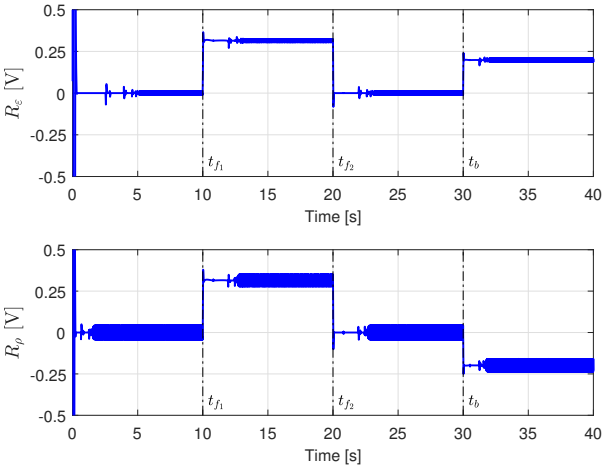

Fig. 8. Fault detection with ST control.

compensated exactly by the ST controller. The controllers u_s in (8) and u_d in (9) are drawing in Fig. 7. There are proportional changes in the magnitude of the controllers when any fault occurs.

The residual equations (15) and (16) are shown in Fig. 8. It can be note when a fault occurs in the front motor (interval T_f) both residual equations have the same magnitude and sign. On the other hand, when a fault occurs in the back motor (at the time t_b until the end) both residual equations have the same magnitude but opposite sign. In addition, the residual equations are mostly affected by discretization noise when the CT controller is used instead of the ST.

3) Analysis of the Simulation Results: The simulations done for the ST and the CT controllers allows to conclude the following:

1. Both controllers are able to compensate exactly the faults in the front motor or in the back motor.
2. The residual equations have the same magnitude in presence of any fault, but when a fault occurs in the front motor the residuals have the same sign and when a fault occurs in the back motor the residual have opposite sign. Table III summarizes the value of the residual equations in presence of faults.
3. The proposed scheme allows to detect an exact compensate faults in the motors of the 3-DOF Helicopter using continuous control.

VI. CONCLUSIONS

Two Sliding Mode controllers are designed to stabilize a 3-DOF helicopter and a FDI scheme based on residual equations, including third-order differentiators, is proposed. Different faults on the actuation system are induced, to verify the effectiveness of the proposed method. Faults are easily

TABLE III
RESIDUAL EQUATIONS IN PRESENCE OF FAULTS.

Residual	$V_f^* = \gamma_f V_f$	$V_b^* = \gamma_b V_b$
R_ε	$-(1-\gamma_f)V_f$	$-(1-\gamma_b)V_b$
R_ρ	$-(1-\gamma_f)V_f$	$(1-\gamma_b)V_b$

identified with both controllers but partially only the CTA controller is able to compensate for faults.

REFERENCES

[1] X. Qi, D. Theilliol, J. Qi, Y. Zhang, and J. Han, "A literature review on fault diagnosis methods for manned and unmanned helicopters," in *Unmanned Aircraft Systems (ICUAS), 2013 International Conference on*. IEEE, 2013, pp. 1114–1118.

[2] J. C. da Silva, A. Saxena, E. Balaban, and K. Goebel, "A knowledge-based system approach for sensor fault modeling, detection and mitigation," *Expert Systems with Applications*, vol. 39, no. 12, pp. 10 977 – 10 989, 2012. [Online]. Available: http://www.sciencedirect.com/science/article/pii/S0957417412004964

[3] W. Z. L. L. S. B. Yang D, Ren Y, "A novel logic-based approach for failure modes mitigation control and quantitative system reliability analyses," *Maintenance and Reliability (Eksploatacja i Niezawodnosc)*, vol. 17, no. 1, pp. 100–106, 2015.

[4] J. Chen and R. Patton, *Robust Model-Based Fault Diagnosis for Dynamic Systems*. Springer Publishing Company, Incorporated, 2012.

[5] A. Zolghadri, "The challenge of advanced model-based fdir for real-world flight-critical applications," *Eng. Appl. Artif. Intell.*, vol. 68, no. C, pp. 249–259, Feb. 2018. [Online]. Available: https://doi.org/10.1016/j.engappai.2017.10.012

[6] H. Mekki, O. Benzineb, D. Boukhetala, M. Tadjine, and M. Benbouzid, "Sliding mode based fault detection, reconstruction and fault tolerant control scheme for motor systems," *ISA Transactions*, vol. 57, pp. 340 – 351, 2015. [Online]. Available: http://www.sciencedirect.com/science/article/pii/S0019057815000415

[7] C. Edwards, "Sliding mode methods for fault detection and fault tolerant control," *IFAC Proceedings Volumes*, vol. 45, no. 20, p. 1, 2012, 8th IFAC Symposium on Fault Detection, Supervision and Safety of Technical Processes. [Online]. Available: http://www.sciencedirect.com/science/article/pii/S147466701634722X

[8] J. Apkarian, "3-dof helicopter reference manual," *Quanser Consulting Inc, Canada*, 2006.

[9] V. Torres-González, T. Sanchez, L. M. Fridman, and J. A. Moreno, "Design of continuous twisting algorithm," *Automatica*, vol. 80, pp. 119–126, 2017.

[10] E. Capello, E. Punta, and L. Fridman, "Strategies for control, fault detection and isolation via sliding mode techniques for a 3-dof helicopter," in *Decision and Control (CDC), 2016 IEEE 55th Conference on*. IEEE, 2016, pp. 6464–6469.

[11] A. Levant, "Sliding order and sliding accuracy in sliding mode control," *International Journal of Control*, vol. 58, no. 6, pp. 1247–1263, 1993. [Online]. Available: https://doi.org/10.1080/00207179308923053

[12] ——, "Higher-order sliding modes, differentiation and output-feedback control," *International journal of Control*, vol. 76, no. 9-10, pp. 924–941, 2003.

[13] D. Hernández, F. Castanos, and L. Fridman, "Pole-placement in higher-order sliding-mode control," *IFAC Proceedings Volumes*, vol. 47, no. 3, pp. 1386–1391, 2014.

[14] C. Edwards, S. K. Spurgeon, and R. J. Patton, "Sliding mode observers for fault detection and isolation," *Automatica*, vol. 36, no. 4, pp. 541–553, 2000.

[15] H. Rios, C. Edwards, J. Davila, and L. Fridman, "Fault detection and isolation for nonlinear systems via hosm multiple-observer," *IFAC Proceedings Volumes*, vol. 45, no. 20, pp. 534–539, 2012.

[16] R. Isermann, "Process fault detection based on modeling and estimation methodsa survey," *automatica*, vol. 20, no. 4, pp. 387–404, 1984.

[17] W. Chen and M. Saif, "Actuator fault diagnosis for uncertain linear systems using a high-order sliding-mode robust differentiator (hosmrd)," *International Journal of Robust and Nonlinear Control*, vol. 18, no. 4-5, pp. 413–426, 2008.

[18] H. Ríos, E. Punta, and L. Fridman, "Fault detection and isolation for nonlinear non-affine uncertain systems via sliding-mode techniques," *International Journal of Control*, vol. 90, no. 2, pp. 218–230, 2017.

[19] J. Marzat, H. Piet-Lahanier, F. Damongeot, and E. Walter, "Model-based fault diagnosis for aerospace systems: a survey," *Proceedings of the Institution of Mechanical Engineers, Part G: Journal of Aerospace Engineering*, vol. 226, no. 10, pp. 1329–1360, 2012. [Online]. Available: https://doi.org/10.1177/0954410011421717